NASA TECHNICAL NOTE

NASA TN D-6328

LONGITUDINAL INSTABILITY LIMITS WITH A VARIABLE-LENGTH HYDROGEN-OXYGEN COMBUSTOR

by C. Joe Morgan and Daniel E. Sokolowski

Lewis Research Center
Cleveland, Ohio 44135

NATIONAL AERONAUTICS AND SPACE ADMINISTRATION • WASHINGTON, D. C. • APRIL 1971

1. Report No.	2. Government Accession No.	3. Recipient's Catalog No.
NASA TN D-6328		

4. Title and Subtitle	5. Report Date
LONGITUDINAL INSTABILITY LIMITS WITH A VARIABLE-LENGTH HYDROGEN-OXYGEN COMBUSTOR	April 1971
	6. Performing Organization Code

7. Author(s)	8. Performing Organization Report No.
C. Joe Morgan and Daniel E. Sokolowski	E-5759
	10. Work Unit No.
9. Performing Organization Name and Address	731-11
Lewis Research Center National Aeronautics and Space Administration Cleveland, Ohio 44135	11. Contract or Grant No.
	13. Type of Report and Period Covered
12. Sponsoring Agency Name and Address	Technical Note
National Aeronautics and Space Administration Washington, D.C. 20546	14. Sponsoring Agency Code

15. Supplementary Notes

16. Abstract

An experimental investigation determined the longitudinal-mode instability characteristics of a 10 000 pound (44 500-N) thrust, 300-psi (2.068-MN/m^2) chamber pressure, hydrogen-oxygen engine that could be continuously stroked in length from 19 to 65 inches (48.3 to 165.1 cm) during operation. A baffle was used to inhibit the transverse modes. Increasing baffle length stabilized the longitudinal mode of instability. Decreasing the hydrogen-injection temperature was destabilizing. The data were analyzed with the sensitive time-lag theory to determine values of the interaction index n and sensitive time lag τ at the stability boundaries. Values of n and τ increased as the hydrogen-injection temperature decreased. The value of n was dependent on the amplitude of the instability.

17. Key Words (Suggested by Author(s))	18. Distribution Statement
Longitudinal mode instability Combustion instability Hydrogen-oxygen rocket engine	Unclassified - unlimited

19. Security Classif. (of this report)	20. Security Classif. (of this page)	21. No. of Pages	22. Price*
Unclassified	Unclassified	21	$3.00

*For sale by the National Technical Information Service, Springfield, Virginia 22151

LONGITUDINAL INSTABILITY LIMITS WITH A VARIABLE-LENGTH HYDROGEN-OXYGEN COMBUSTOR

by C. Joe Morgan and Daniel E. Sokolowski

Lewis Research Center

SUMMARY

An experimental investigation was made to determine the longitudinal-mode instability characteristics of a 10 000-pound (44 500-N) thrust, 300-psia (2.068-MN/m^2) chamber pressure, hydrogen-oxygen engine. The combustor length could be continuously varied from 19 to 65 inches (48.3 to 165.1 cm) during operation. Increasing chamber length caused the combustion to change from stable to unstable operation at a critical length. As chamber length further increased, the combustion returned to stable operation at a larger critical length. Decreasing the hydrogen-injection temperature increased the total change in length between the two critical lengths.

A three-spoke baffle was used to inhibit transverse mode of instability. Increasing the baffle length was stabilizing to the longitudinal mode of instability.

The experimental stability limits (critical lengths at which instability or stability was encountered as the length increased) were analyzed with the sensitive time-lag theory. The sensitive time lag τ and interaction index n at the stability boundary increased as the hydrogen-injection temperature was decreased. The value of the interaction index was dependent on the amplitude of the instability.

INTRODUCTION

The objective of liquid-rocket-engine stability studies has been to provide the engine designer with information to insure that each engine designed will be stable. Many engines are so large that full-scale experiments are far too expensive. As a result, experimental studies on small-scale engines are used to guide the design for the full-scale engine. The high-frequency stability of an engine cannot always be predicted, however, from these experimental results.

There has been a concerted effort in recent years to experimentally determine the transverse-mode combustion instability characteristics of rocket engines using the hydrogen-oxygen propellant combination. The bulk of the experimental results has been obtained with a 20 000-pound (88 960-N) thrust engine (ref. 1). Some isolated results are also available at 50 000-pound (222 400-N) thrust (ref. 2) and 1 500 000-pound (6.672-MN) thrust (ref. 3). The stability of hydrogen-oxygen engines was shown to be directly related to the hydrogen-injection temperature. As the temperature was decreased, the engines became more unstable. These studies determined the effects of such variables as chamber pressure, propellant weight flow per element, injection distribution, chamber length and diameter, nozzle contraction ratio, and others on the hydrogen temperature at which transverse-mode instability was encountered.

In many engine systems longitudinal-mode instabilities are also observed. The purpose of this investigation was to determine the longitudinal stability characteristics of a hydrogen-oxygen engine at different hydrogen-injection temperatures as a continuous function of chamber length. The investigation used a 10 000-pound (44 500-N) thrust engine with a chamber pressure of 300 psia (2.068-MN/m^2) and a fixed oxidant-fuel ratio of 5. It could be continuously stroked in combustor length from 19 to 65 inches (48.3 to 165.1 cm) to provide a length to diameter ratio variation of 1.8 to 6.0. A three-spoke baffle was mounted on the injector face to eliminate transverse-mode instability.

In order for the engine designer to use the results of this investigation, it was desirable to use a theoretical model to analyze the data. Thus, the theory could be used to extrapolate the data to other engine conditions. The most general stability theory available is the sensitive time-lag theory (ref. 4). Therefore, the sensitive time-lag theory was used to determine how values of pressure interaction index n and pressure sensitive time lag τ change with changes in the hydrogen-injection temperature.

In an earlier work (ref. 5), the interaction index and sensitive time-lag values for combustors using propellants other than hydrogen and oxygen were determined from longitudinal-mode instability characteristics of the combustors. A similar approach was taken in this investigation using hydrogen and oxygen propellants. The pertinent variable of this approach is the chamber length that defines the separation between stable combustion and unstable combustion as chamber length is changed.

SYMBOLS

a speed of sound, ft/sec (m/sec)

f frequency, Hz

L chamber length, ft (m)

M chamber Mach number

m mode number, m = 1 for first longitudinal, m = 2 for second longitudinal

n dimensionless pressure interaction index

T dimensionless pressure sensitive time lag

γ ratio of specific heats

τ pressure sensitive time lag, sec

μ stretched time lag, defined in ref. 12

ω dimensionless oscillation frequency, $\omega = 2\pi fL/a$

Subscripts:

e experimentally determined values

1 stability boundary value at smaller length

2 stability boundary value at larger length

APPARATUS

Engine

The test engine is shown schematically in figure 1. It consisted of (1) a cylindrical combustion chamber with a 10.8-inch (27.4-cm) diameter, (2) an exhaust nozzle formed by a flat plate on the end of the chamber, and (3) an injector mounted on a propellant-transfer tube assembly, which was fixed to the test stand. The cylindrical chamber had a sliding fit over the injector and over the propellant-transfer tube. The annular volume between the propellant-transfer tube and the chamber wall pipe was filled with water. A plastic seal at the injector and an O-ring seal at the propellant-transfer tube contained the water under pressure. The 300-psia (2.068-MN/m^2) combustion pressure acting against the flat-plate nozzle provided sufficient force to discharge the water from this volume through a discharge valve. In this way, the chamber length could be continuously stroked during engine operation through a distance limited by the propellant-transfer tube length of 24.7 inches (62.7 cm). The chamber lengths tested covered a range from 19 to 65 inches (48.3 to 165.1 cm). The combustion length ramp rate was controlled by a valve to about 15 inches per second (38.1 cm/sec).

The flat-plate nozzle was chosen for its minimum damping effect on longituninal modes of instability (ref. 6). The nozzle contraction ratio was 3.0, and the nozzle throat had a 0.25-inch (0.635-cm) radius of curvature. The nozzle was mild steel coated with 0.012 inch (0.0305 cm) of Nichrome and 0.018 inch (0.0457 cm) of zirconium

oxide. The chamber wall was plain carbon steel with 0.003 inch (7.62×10^{-5} m) nickel coating on the hot-gas side. These coatings permitted a test duration of about 3 seconds.

Test Facility

The Rocket Engine Test Facility of the Lewis Research Center (ref. 7) was used. Figure 2 shows the test engine mounted vertically on the test stand of this facility. The nozzle end of the engine can be seen through the Plexiglass window of the stand. The propellant-transfer tube is visible at the top of the stand with the hydrogen manifold and oxygen supply line feeding it. The combustion chamber wall is shown with the water dump line out the upper end. Two large counterweights were used to balance the weight of the chamber wall.

Injector

The injector faceplate was a copper heat-sink type. The concentric-tube injector elements were the same as those used in references 1, 2, and 8. Element details are shown in figure 3. The oxygen orifice diameter was 0.052 inch (0.132 cm), the outer diameter of the oxygen tube was 0.125 inch (0.318 cm), and the hydrogen annulus outer diameter was 0.172 inch (0.437 cm). The injector originally had 397 elements arranged on 11 concentric circles as shown in figure 4. Within each of those circles, the elements were equally spaced. This gave an element radial distribution (ref. 2) of 60 percent.

In preliminary tests, transverse-mode instability occurred; therefore, a three-spoke baffle was added to the injector face. The baffle design provided three equivolume cavities and adequately suppressed the transverse modes. Three lengths of baffle were tested to determine the influence of the baffle on longitudinal instability: 3, 4, and 6 inches (7.6, 10.2, 15.2 cm). Placement of the baffle plugged 46 of the element oxidizer tubes; these are shaded in figure 4. The remaining 351 elements were unchanged.

Instrumentation

Placement of the pressure transducers was selected to determine the character and phase relation of the oscillating pressure field. Two were located in the same radial plane, 135° apart and 3.25 inches (8.3 cm) from the injector face at the start of a run. A third was located 4 inches (10.2 cm) farther downstream and in line with one of the

other two. The response of the transducers was flat to within 10 percent to a frequency of 6000 hertz and had a nominal resonant frequency of about 20 000 hertz in the water-cooled mount. The output of these transducers was recorded on magnetic tape. Details of instrumentation associated with the facility are given in reference 7.

TEST PROCEDURE

Before a test, the annular volume between the propellant-transfer tube and the chamber wall was filled with water. This caused the chamber wall to slide relative to the injector, thereby shortening the combustion chamber length. The engine was started and on reaching steady-state operation, the water-discharge valve was opened. The test was terminated when the chamber reached its maximum length. To define a map of stability boundaries, each test was made at a different, but fixed, hydrogen-injection temperature. The hydrogen temperature was varied down to about 55° R (31 K) by mixing given amounts of liquid and gaseous hydrogen. A detailed description of the hydrogen temperature controller is given in reference 7. The oxidant-fuel ratio was maintained in all tests at about 5.0.

Data Recording and Retrieval

It was desirable to compare the amplitude and frequency of the experimental pressure oscillations with theoretical results. Therefore, the chamber pressure history at each transducer location was FM recorded on magnetic tape at 60 inches per second (1.524 m/sec). A 1000-hertz time code was also recorded on the tape to provide the precise locations of pertinent data. The data of interest were retrieved at an effective playback speed of 1280 inches per second (32.51 m/sec) and recorded on an oscillograph. The fundamental frequency of the oscillation during transition from stable to unstable operation was obtained by band passing the pressure history of interest to obtain the fundamental frequency and then electronically converting this wave-form to a square wave. This technique enhanced the ability to read the period of the oscillation when the oscillation amplitude was very small.

RESULTS AND DISCUSSION

A typical test to determine stability boundaries as chamber length was increased is shown in figure 5. The combustion chamber length was increased from 20 to 45 inches

(50.8 to 114.3 cm) during the test. This caused the combustion pressure to go from a steady-state value near 300 psia (2.068 MN/m^2) to an unstable amplitude of 150 psid (1.034 MN/m^2), peak-to-peak, at a length of about 29.5 inches (74.9 cm). The instability continued (except for some short stable periods) until about 40.7 inches (103.4 cm). The combustion again stabilized to a steady-state amplitude of 300 psia (2.068 MN/m^2). Combustion continued to the 45-inch (114.3 cm) length. The frequency of the instability corresponded to the first longitudinal mode. This procedure was repeated to determine stability boundaries (lengths at which instability was first encountered and when it disappeared) at various hydrogen-injection temperatures and with various baffle lengths.

Stability Results

The stability boundaries determined from tests with a 3-inch (7.6-cm) long baffle are shown in figure 6. The open symbols are the hydrogen-injection temperature and combustion chamber length at which the combustion became unstable (or stable) as chamber length was increased. The shaded symbols, which represent values at the end of a stroke, indicate that the combustion remained unstable at the greatest attainable length for that particular test. The eventual transition from unstable to stable combustion, therefore, would occur at some greater chamber length. Above 82° R (46 K), no instability was observed. Below 82° R (46 K), the mode of instability was the first longitudinal for chamber lengths near 30 inches (76.2 cm) and second longitudinal at lengths near 60 inches (152.4 cm). In the region from 32 inches to 50 inches (81.3 to 127 cm), the boundary was not defined. However, as figure 7 shows, the dashed-line boundary is consistent with tests of the 4-inch (10.2-cm) baffle to be discussed.

The instability regions widen as the hydrogen-injection temperature is decreased. In terms of the total range of chamber lengths and hydrogen temperatures, it was destabilizing to decrease the hydrogen-injection temperature. This result is consistent with the results involving transverse instability in hydrogen-oxygen engines (ref. 7).

The influence of an axial baffle on longitudinal modes of instability would be expected to be negligible based on the percent cross-sectional area change of 3.3 percent of the combustion chamber at the injector end. To examine this hypothesis, baffle length was varied and the results are shown in figure 7.

Increasing the baffle length dropped the stability boundary to lower hydrogen-injection temperatures. It was concluded, therefore, that the presence of axial baffles does influence longitudinal-mode instability and that unstable regions diminish in size as length is increased from 3 to 6 inches (7.6 to 15.2 cm).

Theoretical Analysis

The sensitive time-lag theory was used to analyze the experimental results shown in figure 7. Values of the sensitive time lag and interaction index were calculated following the procedure described in the appendix. For a fixed hydrogen injection temperature, the sensitive time lag and interaction index were calculated from the two data points where instability was first observed and when it disappeared. Since the injector, flow rate, and operating conditions did not change as the length increased, it was assumed that, during stable operation (or very low amplitude oscillation), (1) the combustion process remained constant and (2) the absolute value of the interaction index and sensitive time lag remained constant.

Figure 8 shows the values of interaction index and sensitive time lag determined from the curves in figure 7. The interaction index n_e increased as the hydrogen-injection temperature was decreased. This is destabilizing in that it would cause a stable combustion process to be closer to the stability boundary (or an unstable combustion process to be deeper into the instability) as can be seen on figure 9. Similarly, the sensitive time lag τ_e increases as hydrogen-injection temperature is decreased.

Decreasing the baffle length at a given hydrogen-injection temperature also increases the n_e (fig. 8). The time lag increased as baffle length was decreased. It seems that the curves of figure 8 are normally displaced in direct proportion to baffle length.

The effect of the presence of baffles in the combustion chamber is not included in the theory used to determine the values of n_e and τ_e in figure 8. Therefore, the results shown in figure 8 may not represent the effect of baffle length on the sensitive time lag and interaction index at all. If the baffle had no effect on the combustion process, the effect of a baffle change from 3 to 6 inches (7.6 to 15.2 cm) would require a change in the minimum n theoretical value of about 10 percent and the τ theoretical value (at minimum n) of about 15 percent.

A postulated path of a typical test is shown in figure 9. At chamber lengths between 22 and 30 inches (55.9 and 76.2 cm), the combustion pressure oscillation was only low-amplitude noise. At a chamber length of 30 inches (76.2 cm), the oscillation changed from noise to noise superimposed with a sinusoidal oscillation. As the length increased, the sinusoidal oscillation quickly developed into a high-amplitude shock wave. At a chamber length near 41 inches (104.1 cm) the instability decayed quickly to a sinusoidal oscillation to noise again. The low-amplitude noise oscillations continued from 41 to 45 inches (104.1 to 114.3 cm). The n_e at the stability boundary (30 and 41 in. or 76.2 and 104.1 cm) was determined to be 0.50 (see fig. 8). The shock-wave instability at an amplitude of 150 psid (1.034 MN/m^2) corresponded to an n_e of about 0.58. Thus, there is a nonlinear effect of amplitude on n_e.

The actual path of the combustion parameters is not known. Some possible causes for this behavior as postulated are that the presence of the oscillating pressure field may change the combustion response by changing the drop size produced (ref. 9) or by changing the atomization rate (ref. 10) due to the inherent velocity field produced by the oscillation of pressure.

The transition from stable operation to shock-wave instability took place within a few cycles of oscillation. Figure 10 shows a typical transition. As chamber length increased (with time), the pressure oscillations changed from noise (amplitude of 20 psid (1.379×10^5 N/m^2)) to a sinsoidal wave to a shock wave (amplitude of 125 psid (8.618×10^5 N/m^2)). Theory indicates that this kind of transition will take place at an n_e less than about 0.58 (see fig. 9). All values of n_e at the critical stability lengths were below 0.58 (see fig. 8).

The other transition, from shock-wave instability to stable combustion, was not so clearly defined. For example, figure 11 shows three tests with various spurts of instability near this transition. The transition length used to define the stability boundary was taken to be the last transition from unstable operation.

Comparisons of theoretical and experimental shock-wave forms showed that a determination of combustion parameters from the wave characteristics is very unlikely. Figure 12 shows a comparison of an experimental waveform with a corresponding theoretical waveform (transformed according to ref. 11 to distort the wave analogous to the recording system distortion expected during the test). Reference 12 shows that the location of a negatively infinite slope, relative to the shockwave in the pressure-time record, is needed to determine τ_e. It is apparent that a matching of detail such as this is impossible.

The longitudinal mode instability shown in figure 10 had a superimposed oscillation of low-amplitude, third tangential-mode frequency. This shows that the baffle did not completely eliminate transverse modes.

SUMMARY OF RESULTS

The following results were obtained with a variable-length hydrogen and oxygen rocket engine which was stroked during operation to continuously vary the combustion chamber length:

1. As the chamber length was increased, the mode of operation changed from initially stable to unstable in the first longitudinal mode at a critical length and then became stable again at a second critical length. At still longer chamber lengths, the second longitudinal mode was encountered.

2. Decreasing the hydrogen-injection temperature was destabilizing to the longitudinal modes of instability.

3. Baffles suppressed but did not completely eliminate the tangential modes of instability, and they stabilized the longitudinal mode of instability as their length was increased.

4. Decreasing hydrogen-injection temperature increased the sensitive time lag and the interaction index.

5. The unstable oscillation was characterized by a shock wave. The interaction index depended on the amplitude of the shock.

Lewis Research Center,
National Aeronautics and Space Administration,
Cleveland, Ohio, December 30, 1970,
731-11.

APPENDIX - DETERMINATION OF COMBUSTION STABILITY PARAMETERS

Theoretical treatments of combustion instability are of two types: linear and nonlinear. The linear treatment is mathematically more simple and is often described as a solution of the fundamental equations in linearized form. The results of linear analysis describe only the stability boundary. Nonlinear analysis is needed to describe the conditions (such as amplitudes of combustion pressure, density, and temperature as functions of time and distance down the chamber) that occur within the stability boundary) and nonlinear results will be reviewed separately.

Fundamental to theoretical developments of combustion instability is a model to represent the response of the combustion process to assumed perturbations. The sensitive time-lag model of combustion response identifies two parameters to represent this response: an index of interaction n and a time lag τ (ref. 6). It is assumed that the combustion process can be correlated with the instantaneous pressure. The ratio

$$\frac{\text{fractional change of combustion rate}}{\text{fractional change of pressure}} = n\left(1 - \exp\frac{-i\omega\tau a}{L}\right)$$

is then determined. A justification of this formulation is given in reference 13. The combustion parameters n_e and τ_e that correspond to a particular combustion process must be obtained from comparisons of experiment and theory. Three methods are suggested in references 5 and 12 to determine n_e and τ_e: (1) transition frequency with the linear theory, (2) chamber length at transition with the linear theory and (3) waveform properties of the unstable pressure oscillation with the nonlinear theory. Only the second method was successful in this study.

Linear Theoretical Results

Figure 13 shows the stability map determined from reference 12 (for $\gamma = 1.2$ and $M = 0.22$) for the linear (low amplitude sinusoidal) boundaries of the first and second longitudinal modes. Reference 12 assumes concentrated combustion at one end of the combustion chamber and a short nozzle at the other end with the following result on the stability boundary:

$$n = \frac{\gamma + 1}{2\gamma}\left(\frac{1}{1 - \cos \pi\mu}\right)$$

$$T = \left(\frac{1}{m} + \frac{M\gamma n}{\pi} \sin \pi\mu\right)\mu$$

$$\omega = \frac{m\pi}{1 + \frac{2\gamma Mn}{\pi} \sin \pi\mu}$$

For a given mode of instability, there are two values of sensitive time lag T_1 and T_2 (where $T = \tau a/L$) at each value of n above 0.46 that will provide the transition between unstable and stable (or another unstable mode) operation. For given n and τ (to be determined experimentally as n_e and τ_e) and speed of sound, there will be two chamber lengths of transition L_1 and L_2. As chamber length is increased from a stable value at L_1, the chamber pressure oscillations are predicted to grow in amplitude and are nonlinear. The frequency of oscillation at L_1 depends on the value of n and is slightly below the pure acoustic frequency for this length chamber with hard walls and no flow. As chamber length increases to the larger length L_2, the oscillation frequency decreases. At L_2 the frequency is slightly higher than the pure acoustic frequency for this length chamber. At a chamber length corresponding to a sensitive time lag of 1.0 on the stability boundary, the oscillation frequency is the acoustic frequency obtained with no flow and a solid wall at the throat.

Examination of the experimental transition frequencies showed that measurement error was too large to obtain n and τ values from the transition frequency. Therefore, the method using chamber length at transition was used. In applying the method, the values of n and τ were assumed to be constant during a chamber length change for each hydrogen-injection temperature. The speed of sound (which must be known) was assumed to be constant at 5310 feet per second (134.87 m/sec). With these restrictions,

$$\frac{T_1}{T_2} = \frac{L_2}{L_1}$$

$$\tau = \frac{T_1 L_1}{a} = \frac{T_2 L_2}{a}$$

and

$$n = \text{function of } L_2/L_1$$

Values of n_e and τ_e at the linear stability boundary (low amplitude) are determined for experimental values of L_1 and L_2.

Nonlinear Theoretical Results

Reference 12 is a nonlinear analysis of the longitudinal mode instability. Figure 9 shows the linear and nonlinear stability boundaries for the first longitudinal mode from reference 12 with lines of constant-oscillation amplitude in the unstable region. Shock-wave solutions are obtained within the unstable region. The nonlinear boundary is outside the linear boundary for n greater than 0.58. Between the two boundaries, a pressure pulse could cause a transition to instability via the nonlinear (shock wave) boundary. Otherwise, the transition will take place at the chamber length corresponding to the linear boundary and develop into a shock-wave instability. On the transition out of the instability (caused by increasing chamber length through the stability boundary), the shock-wave amplitude decays.

For n less than 0.58, the transition to a sinusoidal wave occurs at the linear limit. As chamber length increases, the sinusoidal wave grows to a shock wave at the nonlinear limit. The shock wave degenerates to a damped sinusoidal wave at the other boundary. The nonlinear boundary is dependent on the Mach number of the combustion gas flow. Reference 12 shows that the location of a negatively infinite slope (fig. 12), relative to the shock wave in the pressure-time record, would determine τ_e. The n_e would then be determined from the experimental shock amplitude. This method was not successful because of the inability to locate the negatively infinite slope.

REFERENCES

1. Conrad, E. William; Bloomer, Harry E.; Wanhainen, John P.; and Vincent, David W.: Interim Summary of Liquid Rocket Acoustic-Mode-Instability Studies at a Nominal Thrust of 20 000 Pounds. NASA TN D-4968, 1968.

2. Wanhainen, John P.; and Morgan, C. Joe: Effect of Injection Element Radial Distribution and Chamber Geometry on Acoustic-Mode Instability in a Hydrogen Oxygen Rocket. NASA TN D-5375, 1969.

3. Barsotti, R. J.; Datsko, S. C.; Louison, R.; Kovach, R. J.; Miller, D. J.; and Pulliam, W. P.: Development of Liquid Oxygen/Liquid Hydrogen Thrust Chamber for the M-1 Engine. Rep. AGC-9400-5, Aerojet-General Corp. (NASA CR-54813), May 15, 1968.

4. Smith, A. J.; and Reardon, F. H.: The Sensitive Time Lag Theory and Its Application to Liquid Rocket Combustion Instability Problems. Vol. 1. Engineer's Manual. Aerojet-General Corp. (AFRPL-TR-67-314, vol. 1, DDC No. AD-838825), Mar. 1968.

5. Crocco, Luigi; Grey, Jerry; and Harrje, David T.: Theory of Liquid Propellant Rocket Combustion Instability and its Experimental Verification. ARS J., vol. 30, no. 2, Feb. 1960, pp. 159-168.

6. Crocco, Luigi; and Cheng, Sin-I: Theory of Combustion Instability in Liquid Propellant Rocket Motors. AGARDograph 8. Butterworth Scientific Publ., 1956.

7. Wanhainen, John P.; Parish, Harold C.; and Conrad, E. William: Effect of Propellant Injection Velocity on Screech in 20 000-Pound Hydrogen-Oxygen Rocket Engine. NASA TN D-3373, 1966.

8. Wanhainen, John P.; Feiler, Charles E.; and Morgan, C. Joe: Effect of Chamber Pressure, Flow per Element, and Contraction Ratio on Acoustic-Mode Instability in Hydrogen-Oxygen Rockets. NASA TN D-4733, 1968.

9. Heidmann, Marcus F.; and Wieber, Paul R.: Analysis of Frequency Response Characteristics of Propellant Vaporization. NASA TN D-3749, 1966.

10. Heidmann, Marcus F.; and Groeneweg, John F.: Analysis of the Dynamic Response of Liquid Jet Atomization to Acoustic Oscillations. NASA TN D-5339, 1969.

11. Crocker, M. J.; and Sutherland, L. C.: Instrumentation Requirements for Measurement of Sonic Boom and Blast Waves - A Theoretical Study. J. Sound Vibration, vol. 7, no. 3, May 1968, pp. 351-370.

12. Mitchell, Charles E.: Axial Mode Shock Wave Combustion Instability in Liquid Propellant Rocket Engines. Rep. AMS-TR-798, Princeton Univ. (NASA CR-72259), July 1967.

13. Crocco, L.: The Relevance of a Characteristic Time in Combustion Instability. Second ICRPG Combustion Conference. Rep. CPIA Publ. No. 105, Vol. 1, Applied Physics Lab., Johns Hopkins Univ., May 1966, pp. 115-138.

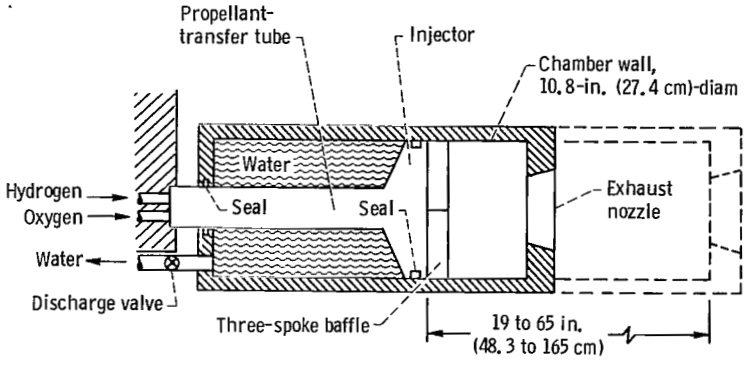

Figure 1. - Test engine showing variable length feature of chamber.

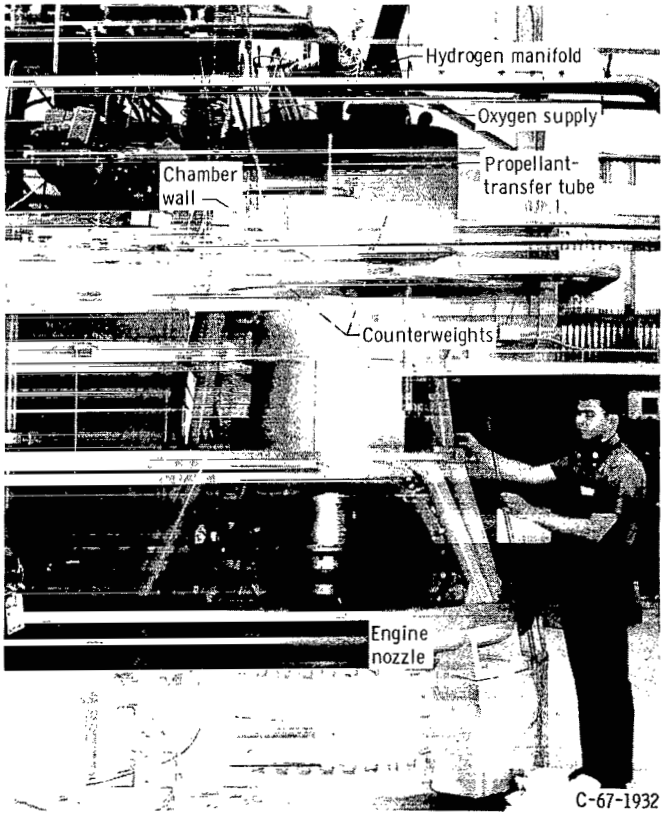

Figure 2. - Test facility showing test engine mounted vertically.

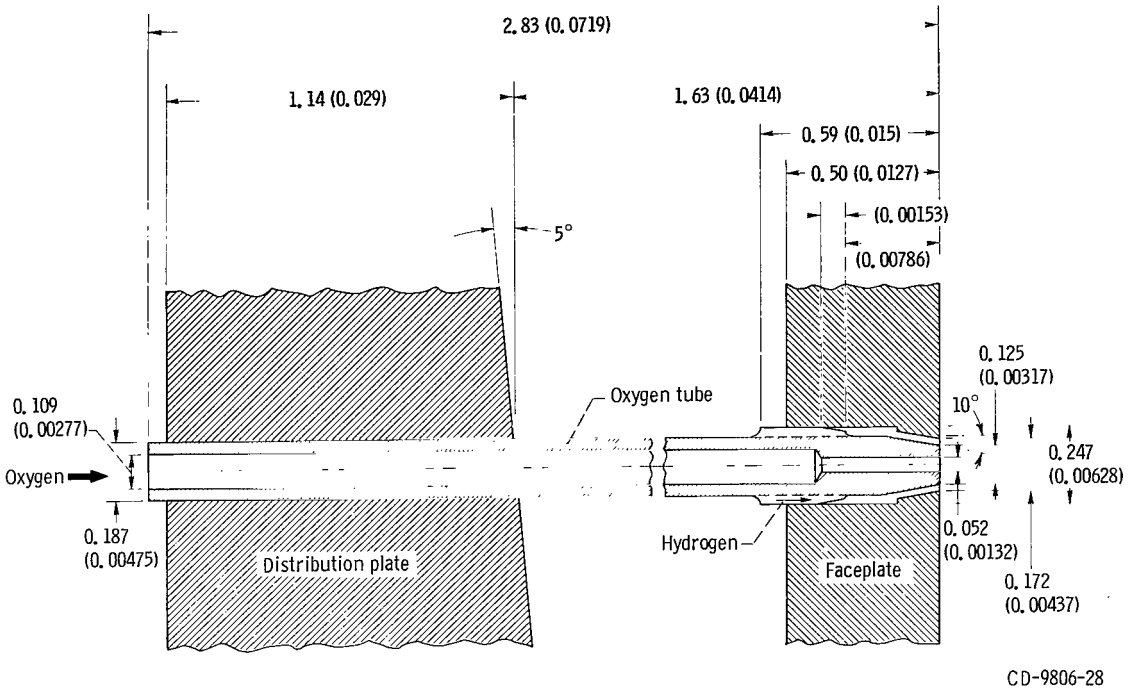

Figure 3. - Concentric tube injector element used in tests.

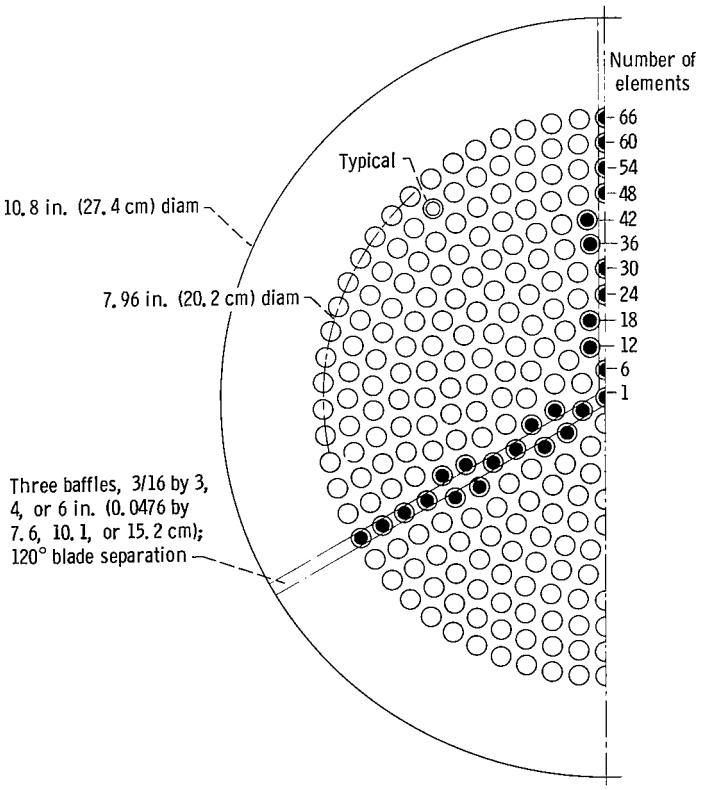

Figure 4. - Injector face pattern showing baffle locations and oxygen tubes that were plugged to accommodate baffles. Elements equally spaced on concentric circles 0.362 inch (0.919 cm) apart. Shaded elements are plugged oxygen outlets.

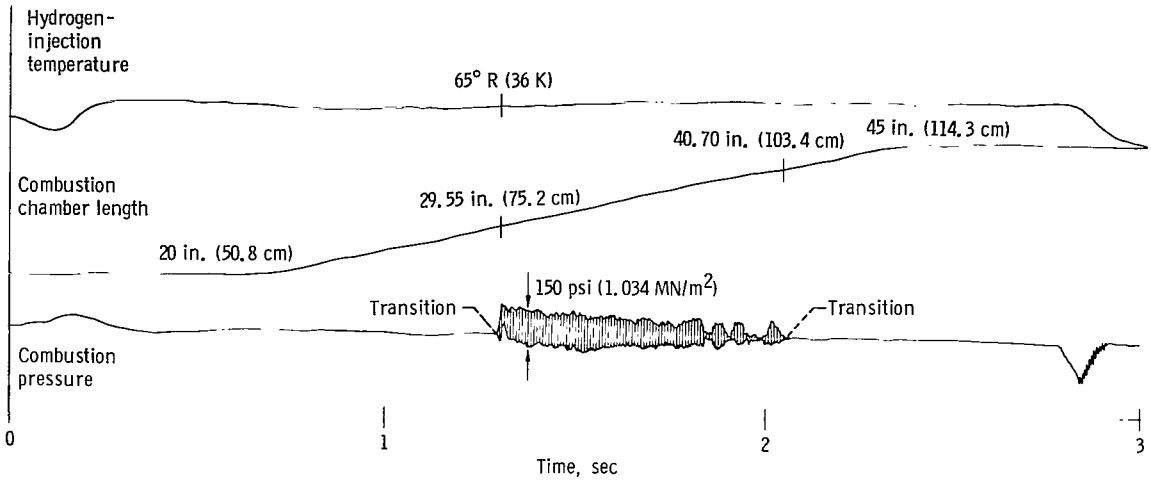

Figure 5. - Oscillograph traces of typical screech test of 4-inch (10.2-cm) baffle test.

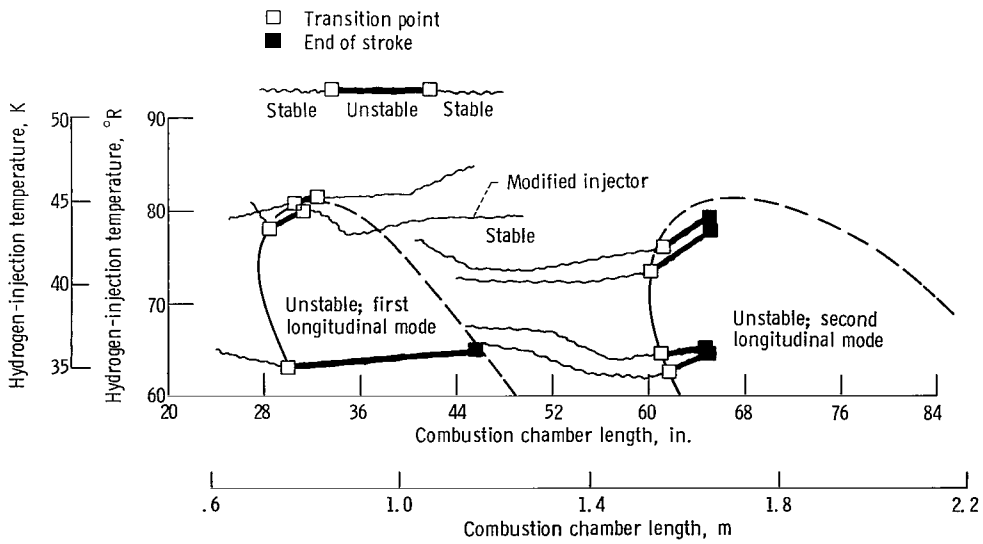

Figure 6. - Experimental stability boundary with 3-inch (7.6 cm) baffle.

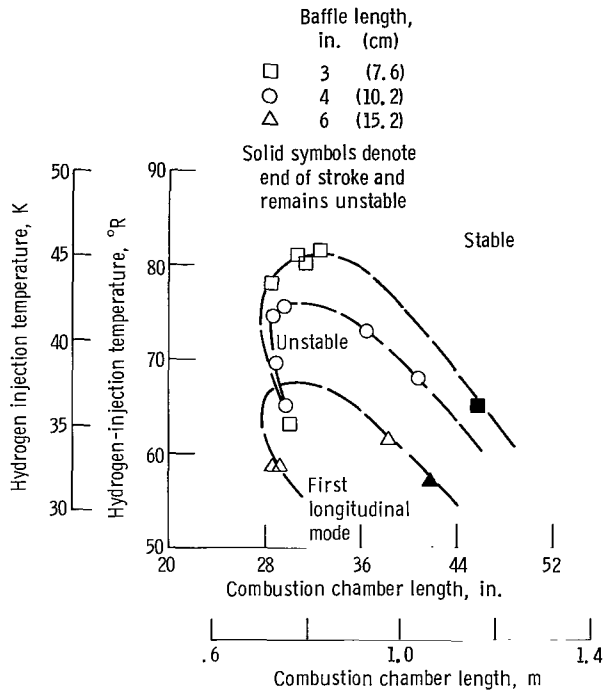

Figure 7. - Experimental stability boundaries with various baffle lengths.

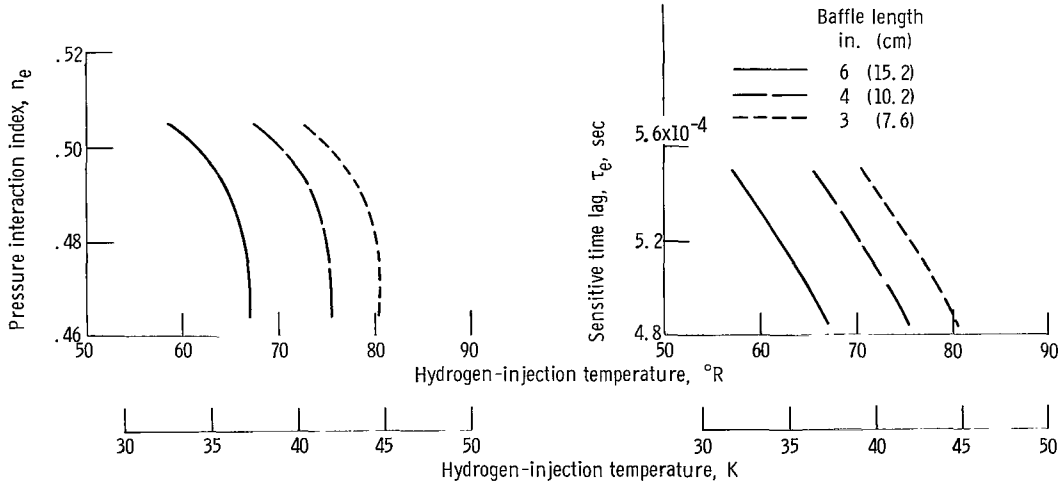

Figure 8. - Experimentally determined combustion parameters on stability boundary.

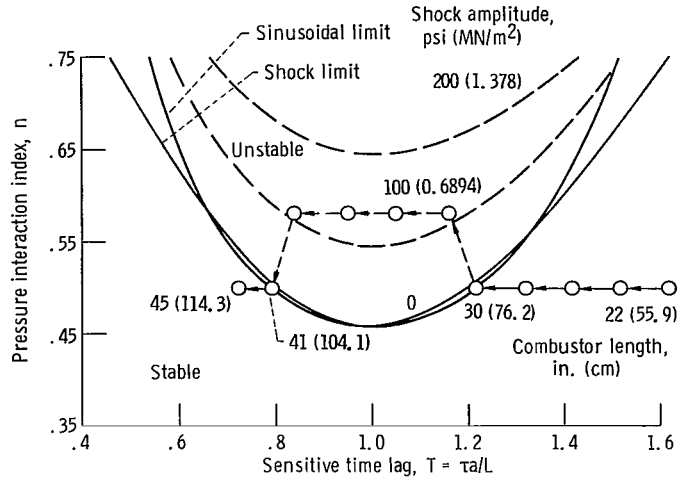

Figure 9. - Postulated path of 4-inch (10.2-cm) baffle test. Mach 0.22; hydrogen temperature, 66° R (37 K).

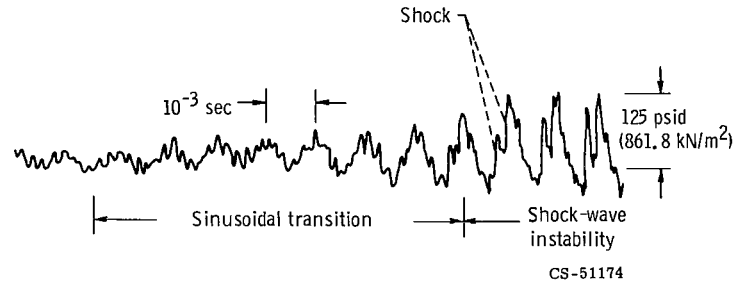

Figure 10. - Pressure history during typical transition into instability. Baffle length, 3 inches (7.6 cm); hydrogen-injection temperature, 63° R (35 K); chamber length, 30 inches (76.2 cm).

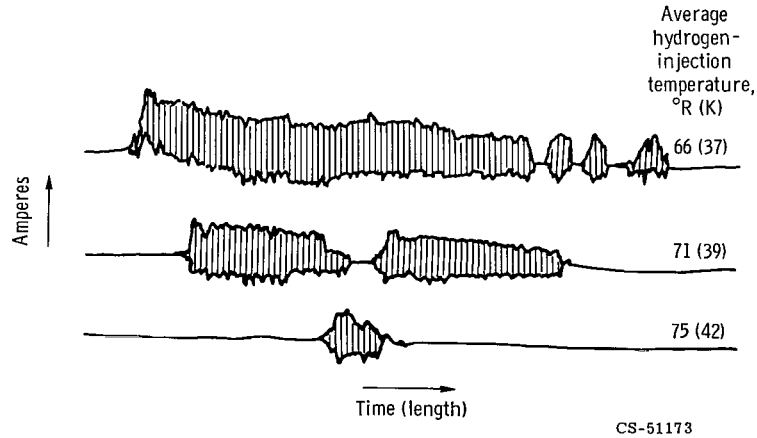

Figure 11. - Form of instability of 4-inch (10.2-cm) baffle tests.

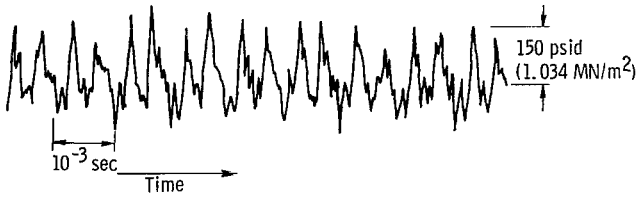

(a) Experimental.

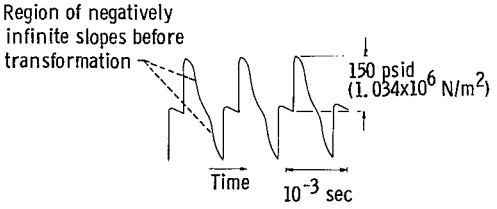

(b) Theoretical. Pressure interaction index, 0.58; dimensionless pressure sensitive time lag, 1.0.

Figure 12. - Comparison of experimental and theoretical instability waves of 4-inch (10.2-cm) baffle test. Hydrogen temperature, 66° R (37 K).

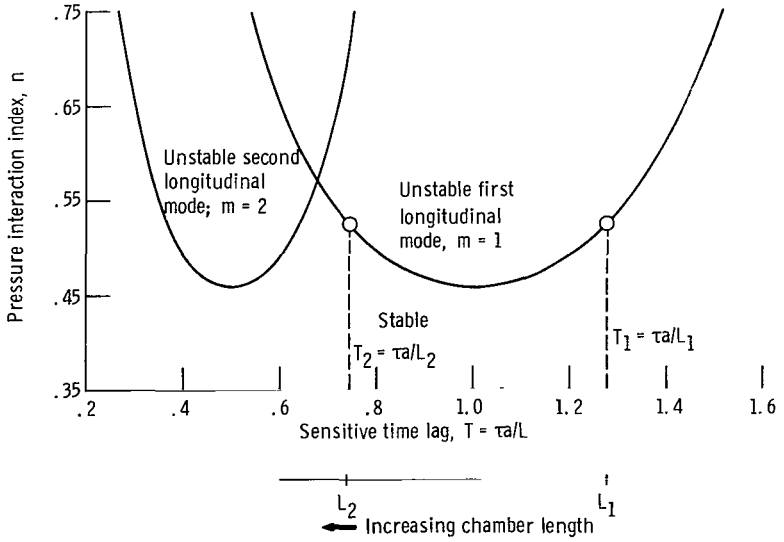

Figure 13. - Linear stability boundaries of longitudinal modes for concentrated combustion and short nozzle. Chamber Mach number, 0.22; ratio of specific heats, 1.2.

06U 001 58 51 3DS 71.10 00903
AIR FORCE WEAPONS LABORATORY /WLOL/
KIRTLAND AFB, NEW MEXICO 87117

ATT E. LOU BOWMAN, CHIEF,TECH. LIBRARY

"The aeronautical and space activities of the United States shall be conducted so as to contribute . . . to the expansion of human knowledge of phenomena in the atmosphere and space. The Administration shall provide for the widest practicable and appropriate dissemination of information concerning its activities and the results thereof."

— NATIONAL AERONAUTICS AND SPACE ACT OF 1958

NASA SCIENTIFIC AND TECHNICAL PUBLICATIONS

TECHNICAL REPORTS: Scientific and technical information considered important, complete, and a lasting contribution to existing knowledge.

TECHNICAL NOTES: Information less broad in scope but nevertheless of importance as a contribution to existing knowledge.

TECHNICAL MEMORANDUMS: Information receiving limited distribution because of preliminary data, security classification, or other reasons.

CONTRACTOR REPORTS: Scientific and technical information generated under a NASA contract or grant and considered an important contribution to existing knowledge.

TECHNICAL TRANSLATIONS: Information published in a foreign language considered to merit NASA distribution in English.

SPECIAL PUBLICATIONS: Information derived from or of value to NASA activities. Publications include conference proceedings, monographs, data compilations, handbooks, sourcebooks, and special bibliographies.

TECHNOLOGY UTILIZATION PUBLICATIONS: Information on technology used by NASA that may be of particular interest in commercial and other non-aerospace applications. Publications include Tech Briefs, Technology Utilization Reports and Technology Surveys.

Details on the availability of these publications may be obtained from:

SCIENTIFIC AND TECHNICAL INFORMATION OFFICE

NATIONAL AERONAUTICS AND SPACE ADMINISTRATION

Washington, D.C. 20546